EUROPEAN COOPERATION
IN THE FIELD OF SCIENTIFIC
AND TECHNICAL RESEARCH

EURO-COST

COST 273 TD(02) 066
Espoo, Finland
2002/May/30-31

SOURCE: INTHF, Technische Universität Wien, Vienna, Austria
Nokia Research Center, Helsinki, Finland

# Spatial Reciprocity of Uplink and Downlink Radio Channels in FDD Systems

Klaus Hugl, Kimmo Kalliola and Juha Laurila

Klaus Hugl
Institut für Nachrichtentechnik
Technische Universität Wien
Gußhausstraße 25/389
A-1040 Vienna
AUSTRIA
Email: Klaus.Hugl@mobile.nt.tuwien.ac.at

Kimmo Kalliola, Juha Laurila
Nokia Research Center
P.O.Box 407
FIN-00045 NOKIA Group
FINLAND
Email: Kimmo.Kalliola@nokia.com, Juha.K.Laurila@nokia.com

# Spatial Reciprocity of Uplink and Downlink Radio Channels in FDD Systems

**Klaus Hugl[1], Kimmo Kalliola[2] and Juha Laurila[2]**

[1]Institut für Nachrichtentechnik und Hochfrequenztechnik (INTHF)
Technische Universität Wien, Vienna, Austria
Klaus.Hugl@mobile.nt.tuwien.ac.at
[2]Nokia Research Center, Helsinki, Finland

***Abstract* - We investigate the congruence of the directional properties of uplink (UL) and downlink (DL) as seen from the base station in WCDMA of UMTS by means of spatial channel measurements. Our study illustrates that the directional properties of the mobile radio channel are strongly correlated in uplink and downlink radio channels. Therefore, the utilization of spatial information derived during uplink reception for downlink smart antenna transmission is reasonable.**

## 1. INTRODUCTION

The application of adaptive antennas in cellular mobile communication systems has raised increased interest during recent years [1]. The introduction of the 3rd generation (3G) mobile communication systems supporting high-data rate services, e.g. video streaming and multimedia applications will create asymmetric traffic in favor of the downlink. Additionally, heavily loaded CDMA systems like UMTS will be downlink interference limited. As a consequence, the improvements that smart antennas can provide are especially required in the downlink.
One way to operate an adaptive antenna base station (BS) without mobile station (MS) feedback in the downlink is to reuse spatial (angular) information derived during uplink reception (e.g. [2]). But a prerequisite for this methodology is that the spatial channel characteristics at the uplink and downlink frequencies are similar.
Different channel sounding campaigns can be found in literature [3-6] that tried to answer whether this assumption also holds in systems applying frequency division duplex (FDD). But the authors of these papers drew controversial conclusions. Therefore, we first comment on the available literature and then present our measurement results.

## 2. STATE OF THE ART

The first investigations of the congruence of uplink and downlink spatial channel characteristics were done by comparing the dominant direction of arrival (DOA) [3]. In the measurement setup the relative duplex distance was limited to <3% (25MHz at 900MHz) which is much less than in W-CDMA (≈10%). Moreover, these results lack statistical reliability because only some stationary transmitter positions were measured. The authors of [3] conclude that the dominant *DOA is relatively stable* in the considered frequency band.

Measurements in Aalborg [4] were performed using a moving transmitter and a duplex distance of 68MHz at a carrier frequency of 1.7GHz. The authors averaged the channel over a distance of 40 wavelengths to overcome small-scale fading effects. They applied the SAGE algorithm [7] to extract the APS and correlated the first central moment of it. The authors concluded that the first central moment of the *APS is very well correlated*.
We would like to mention that the correlation of the first central moment $\overline{\varphi}$ of the APS might have one big drawback: several different APS shapes give the same center of gravity, as illustrated in Fig. 1.

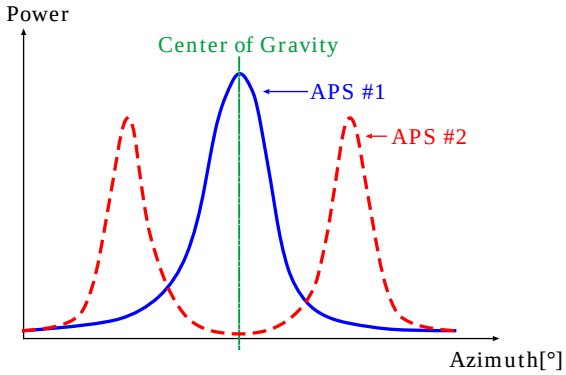


Figure 1: The same center of gravity is obtained by two different APS (in blue and red color).

Moreover, the distribution of the center of gravity $\overline{\varphi}$ in azimuth itself has a strong influence on the derived correlation coefficient even if the deviation $\overline{\varphi}_{UL} - \overline{\varphi}_{DL}$ is the same. If the dominant propagation clusters are located at array broadside ($0<|\overline{\varphi}|<30°$) the correlation coefficient will be lower than for off broadside ($30°<|\overline{\varphi}|<90°$).
Thus, the center of gravity correlation coefficient is an ambiguous measure for the APS shape correlation in uplink and downlink.

Measurements conducted in Bristol [5] were done by performing wideband measurements and extracting the UL and DL frequency band by subband filtering. The measurement bandwidth was 120MHz in the 2GHz band and therefore the maximum possible duplex distance was limited to the measurement bandwidth. Only a few mobile station transmitter positions were monitored. The author(s) concluded that the *APS* of uplink and downlink is *uncorrelated* in cellular mobile communications systems with frequency division duplex. We see the following short-comings of their surprising result.
Samples for each transmitter positions were taken within 10s. Averaging over this time period with a constant transmitter and receiver position does not necessarily guarantee independence of small-scale fading. The directions of arrival were extracted using the Unitary Esprit algorithm [8]. These DOAs were then used to create an artificial antenna array response with a variable number of antenna elements to calculate the APS using the Bartlett beamformer [9].
Strictly speaking, this means the reduction of the spatial information to some discrete parameters (namely the discrete DOAs) to create the continuous azimuth power spectrum. In this way, one looses information which might have affected the given APS correlation of UL and DL.

Recently a follow up measurement campaign was performed in Bristol [6], now sounding the channel at two carrier frequencies performing dynamic drive measurements.
For measurement data evaluation [10] the authors utilized the 2-D Unitary Esprit algorithm to estimate the DOA and the delays of the different multipath components. Moreover, they extracted the complex coefficients (amplitude and phase) of each multipath component. After restricting the dynamic range to 15dB, the APS is calculated with a resolution of 0.5°, as the integral in the delay domain of all complex coefficients lying in a 0.5° wide bin. As a consequence of their APS definition, the "power" (complex coefficient) associated with an azimuth bin is strongly dependent on the phase states of delayed multipath components having nearly the same angle of incidence. Therefore, constructive and destructive superposition of the complex phasors in the delay domain affect the calculated "APS" measure. Finally, they calculated the correlation of their complex valued APS using the angular resolution of 0.5°.
As a consequence of their APS definition using discrete complex valued waves with a 0.5° grid, the APS seems to be uncorrelated on a first look although it is not. Let us now investigate where there are still some pitfalls.

- The integration of the complex coefficients in the delay domain for each frequency band introduces artificial fading. These "fading coefficients" should represent the directional power and will be uncorrelated because of the different carrier frequencies resulting in APS decorrelation. Therefore, two discrete waves with correctly estimated azimuths $\varphi_1$ and $\varphi_2$ but complex phasors

$$\alpha_{1,UL}=\alpha_{1,DL}=\alpha_{2,UL}=-\alpha_{2,DL} \qquad (1)$$

  result in a totally uncorrelated APS as well. The reason for that is only the changing phase due to the different carrier frequencies also if the power and the azimuth angle of the waves are identical.
- The resolution of 0.5° and the discrete wave assumption leads to decorrelation also if the APS from our point of view is correlated. A single DOA estimate with 0.5° estimation deviation in UL and DL results in a correlation coefficient of $\rho=0$. We also have to keep in mind that the estimation reliability is affected by imperfect array and receiver chain calibrations.

Thus, it is not surprising that the authors of [6] state the *APS* to be *uncorrelated*. We recommend to not use complex coefficients and the discrete wave assumption for APS correlation purpose.

In the following sections, we will describe our measurement setup as well as how we estimate the APS and define its correlation.

## 3. MEASUREMENT SETUP

The spatial channel sounding campaign described herein was conducted by Nokia Research Center (NRC) Helsinki in cooperation with INTHF in June 2001 in downtown Helsinki. For measurement purpose the NORPPA channel sounder built by Elektrobit AG [11] was applied.

In the measurements, a vehicular transmitter mounted on the roof of a measurement van at a height of about 2.4m above ground level was used. The sounding signal was either transmitted using a vertically polarized monopole or a dummy handset attached to a phantom head. The measurements were simultaneously performed on an uplink ($f_{UL}$=1935MHz) and downlink carrier ($f_{DL}$=2125MHz) in the UMTS band. A modulated PN-sequence of length 127 and a chip-rate of 5MChips/s was applied as channel sounding signal. We performed dynamic drive measurements with a target speed of 40km/h in the center of Helsinki along different measurement routes. The dynamic drive measurements allow the spatial channel characterization for full BS sector coverage without the lack of limited statistics.

At the receiver/BS position an 8-column uniform linear array (ULA) was used, each column consisting of 4 vertically polarized dipoles. Each column of the physical array has a gain of 11dBi and 3dB-beamwidth of 120° in the horizontal (azimuthal) domain and 18° in the vertical plane. The inter-column distance was $d$=67mm corresponding to $0.432\lambda_{UL}$ and $0.475\lambda_{DL}$. The array was mechanically downtilted by 7°.

The signals of the 8 antenna columns were collected using the fast RF switching technique of [12]. In the receiver 4-times oversampling was applied resulting in a delay resolution of $\Delta\tau$=50ns. A single recorded array channel impulse response $\mathbf{h}(f)$ has a dimension of 8 spatial samples (number of antenna columns) versus 508 delay samples

$$\mathbf{h}(f) = \begin{bmatrix} h_1(0,f) & \cdots & h_1(507\cdot\Delta\tau,f) \\ \vdots & & \vdots \\ h_8(0,f) & \cdots & h_8(507\cdot\Delta\tau,f) \end{bmatrix}. \quad (2)$$

A measurement of a full array channel impulse response at $f_{UL}$ and $f_{DL}$ was performed every 3.6ms. Therefore, at least 3 channel snapshots per wavelength are available while the transmitter was moving along the measurement routes.

The antenna array receiver was placed on six different BS positions in the center of Helsinki. In total, more than $3.5\cdot10^6$ complex array channel impulse responses along the drive routes of more than 140km were collected. For more details on the measurement setup and the propagation environment (especially photos of the measurement environments and maps including the route description) see [13].

## 4. MEASUREMENT EVALUATION

In this section we will investigate the correlation of the spatial propagation characteristics of the mobile radio channel at two different carrier frequencies. In this case, the different carrier frequencies correspond to a single uplink and downlink carrier of the UTRA-FDD system. The spatial propagation parameters we consider are the dominant direction of arrival (DOA) and the azimuth power spectrum (APS).

### 4.1 Congruence of dominant UL/DL DOA

Let us first consider the congruence or difference of the instantaneous dominant direction of arrival at the uplink and downlink carrier. We define the dominant DOA as the direction of maximum output power using the Bartlett beamformer [9]

$$\varphi_{dom}(f) = \arg\max_{\varphi}\left\{\sum_{n=0}^{507}\left|\mathbf{a}^H(\varphi,f)\cdot\mathbf{h}(n\cdot\Delta\tau,f)\right|^2\right\}, \quad (3)$$

where $\mathbf{a}(\varphi)$ and $\mathbf{h}(n\cdot\Delta\tau)$ denote the array steering vector of the ULA and the $n$-th delay sample of the recorded complex channel impulse response, respectively.

The distribution of the difference of dominant UL and DL DOA

$$\varphi_{dom,diff}(f_{UL},f_{DL}) = \varphi_{dom}(f_{UL}) - \varphi_{dom}(f_{DL}) \quad (4)$$

of all measurement routes in all sectors is given in Fig. 2.

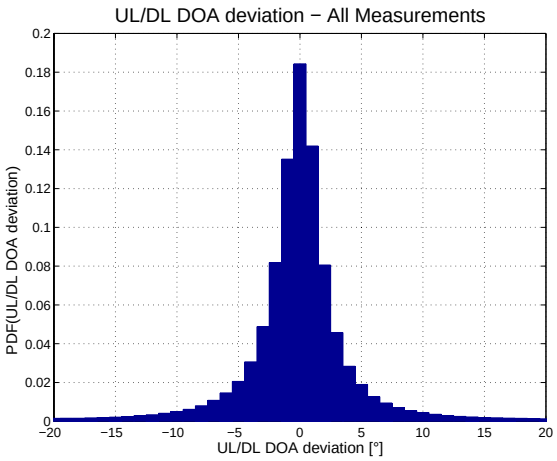


Figure 2: Deviation distribution of the dominant DOA estimated at the UL and DL carrier.

Obviously, there is a nice congruence of the dominant DOA estimated from the recorded channel impulse responses at the uplink and downlink carrier. The remaining deviation is also influenced by spatially selective fading [14]. To mitigate this effect from the measurement data evaluations, we illustrate the deviation of the dominant DOA at uplink and downlink carrier including small scale averaging over 50 consecutive channel snapshots (corresponding to 180ms) in Fig. 3.

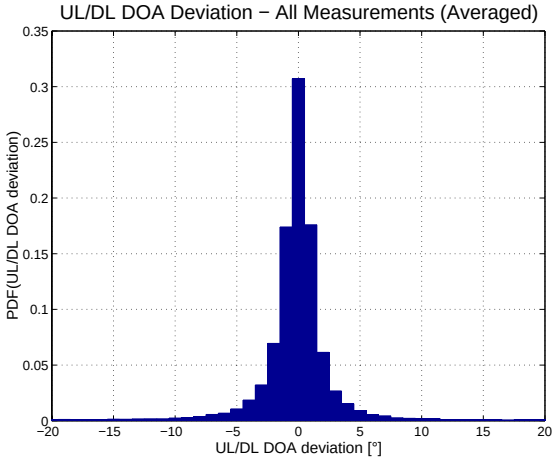


Figure 3: Deviation distribution of the dominant DOA estimated at the UL and DL carrier including small scale averaging.

Obviously, the small scale averaging reduces the deviation even more.

In [15] we have shown, that there is a significant difference in the dominant wave propagation effects for macro- and microcellular BS installations. Thus, we show the UL/DL DOA deviation for the BS installations at the *Helsingin Energia* building from the rooftop (macrocellular) and below the rooftop (microcellular) in Fig. 4 and Fig. 5.

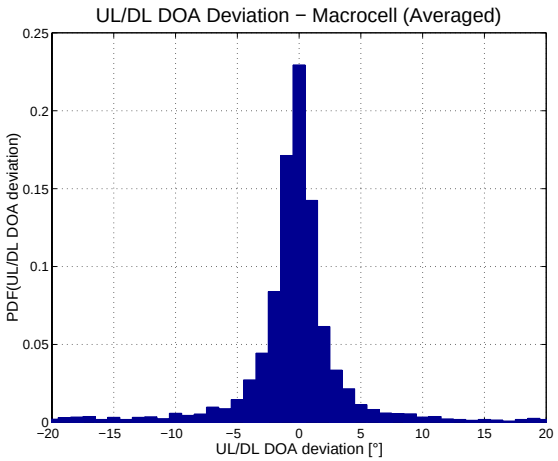


Figure 4: Deviation distribution of the dominant DOA estimated at the UL and DL carrier including small scale averaging. Only the measurement data of the macrocellular BS installation in Sector 160 of the *Helsingin Energia* measurements [13] are utilized.

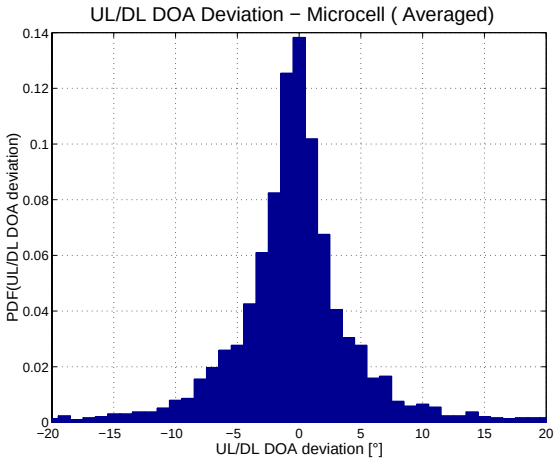


Figure 5: Deviation distribution of the dominant DOA estimated at the UL and DL carrier including small scale averaging (microcellular BS installation in Sector 160 of the *Helsingin Energia* measurements [13]).

Again a nice congruence is visible. For the microcellular BS installation at the balcony of the *Helsingin Energia* building (6.5m below the macrocellular BS installation at the rooftop) the shape of the distribution is slightly wider. The reason for that is the larger angular spreading in the microcellular case due to the relatively large aperture of the street canyons that dominate physical wave propagation. For the macrocell the pseudo-LOS dominates the propagation scenario (shown in [15]) and therefore the small scale averaging is more effective.

In general, the dominant DOA in uplink and downlink show only a minor deviation. Therefore, the utilization of the dominant

DOA estimated during uplink reception for downlink beampointing purpose is reasonable.

### 4.2 Uplink-Downlink APS Correlation

Up to now we only investigated the congruence of the dominant DOA estimated at an uplink and downlink carrier in the UMTS band. But the directional behavior of the mobile radio channel contains much more than just a single DOA. Thus, let us in a second step examine the congruence/correlation of the total azimuth power spectrum (APS).

In section 2, we critically discussed the definitions and results of the same investigations that can be found in literature [4,5,6]. Here we would like to state how we see and define the correlation of the azimuth power spectrum of the uplink and downlink mobile radio channel as seen from a BS antenna array.

For estimation purposes of the APS we use the least-squares power estimator (Capon´s beamformer or Minimum Variance Estimator [16])

$$P(\varphi) = \frac{1}{\mathbf{a}^H(\varphi) \cdot \mathbf{R}^{-1} \cdot \mathbf{a}(\varphi)} \qquad (5)$$

applied on the spatial covariance matrix

$$\mathbf{R} = E_t\left\{\sum_{n=0}^{507} \mathbf{h}(n \cdot \Delta\tau) \cdot \mathbf{h}^H(n \cdot \Delta\tau)\right\}. \qquad (6)$$

This Minimum Variance Estimator produces a smooth estimate of the APS. An angular resolution of 1° inside an azimuthal area of [-70°,70°] from array broadside for the APS $P(\varphi)$ is considered.

The APS is a real and positive valued function in the azimuth $\varphi$. Therefore, the correlation coefficient $\rho$ of instantaneous APS estimates at the frequencies $f_{UL}$ and $f_{DL}$

$$\rho = \frac{\int_{\varphi} P(\varphi, f_{UL}) \cdot P(\varphi, f_{DL})}{\sqrt{\int_{\varphi} P^2(\varphi, f_{UL})} \sqrt{\int_{\varphi} P^2(\varphi, f_{DL})}} \qquad (7)$$

is by definition positive and is only 0 if

$$P(\varphi, f_{UL}) \cdot P(\varphi, f_{DL}) = 0 \qquad \forall \varphi . \qquad (8)$$

This is a consequence of the non-zero mean value of the APS $\overline{P}(f)$. Therefore, we define the APS correlation mathematically correctly as the covariance of the APS

$$\rho = \frac{\int_{\varphi} \left(P(\varphi, f_{UL}) - \overline{P}(f_{UL})\right)\left(P(\varphi, f_{DL}) - \overline{P}(f_{DL})\right)}{\sqrt{\int_{\varphi} \left(P(\varphi, f_{UL}) - \overline{P}(f_{UL})\right)^2} \sqrt{\int_{\varphi} \left(P(\varphi, f_{DL}) - \overline{P}(f_{DL})\right)^2}} . \qquad (9)$$

We do not average the covariance function over several realizations. Instead we plot the distribution of the absolute value of $\rho$ as shown in Fig. 6.

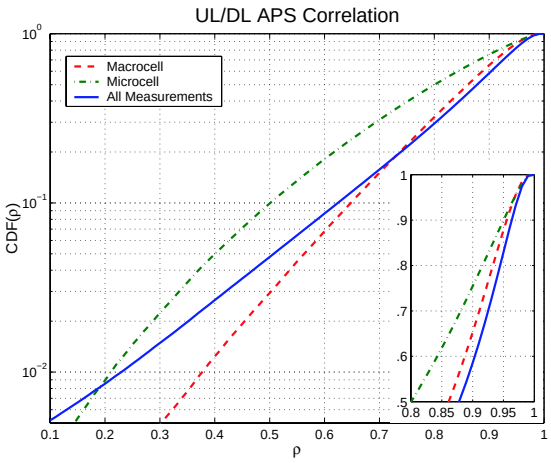


Figure 6: Correlation function of the estimated azimuth power spectrum at the UL and DL carrier.

Obviously, the correlation between the instantaneously estimated APS realizations at $f_{UL}$ and $f_{DL}$ is rather high. In more than 50% of the cases the correlation is higher than 0.8 for the macrocellular as well as the microcellular BS installation. Additionally, we plotted the distribution for all measurements taken in June 2001.

The correlation for the microcellular BS installation is lower than in the macrocellular case. This is again an effect of the street canyon dominated propagation discussed in [15]. The distribution for the macrocellular case described in [13,15] is similar to the distribution of all measurements. The reason is that overall 5 macrocellular but just a single microcellular BS installation was used in this measurement campaign. The distribution of all measurements is dominated for the high correlation values by the macrocellular installations and the lower values are due to the microcellular case.

In Fig. 6 instantaneous estimates of the APS are considered. If several different angular areas (carrying significant power) fade independently, we get decorrelation of the APS due to the uncorrelated fading at the different carrier frequencies. Thus, we consider the APS estimated out of the small-scale averaged spatial covariance matrix in

Fig. 7 (averaging over a time span of 180ms corresponding to 50 consecutive channel snapshots).

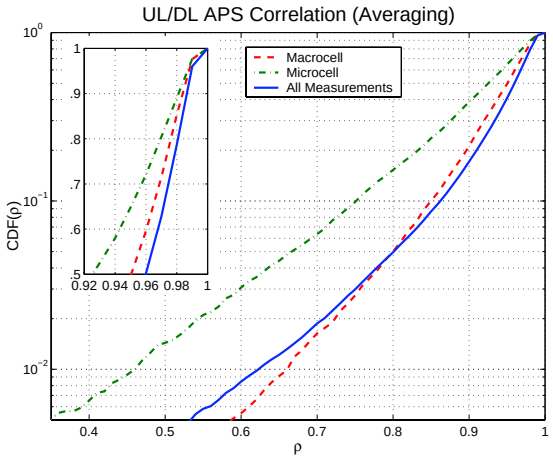


Figure 7: Correlation distribution of the estimated azimuth power spectrum at the UL and DL carrier including small scale averaging.

The small scale averaging mitigating the instantaneous fading situation at the two different carriers improves the correlation even more.

In general we can conclude that the APS in UL and DL as seen from a BS antenna array is very similar.

## 5. SUMMARY AND CONCLUSIONS

We have shown by measurement data evaluation that the spatial behavior seen by an adaptive antenna array at the uplink and downlink carrier of W-CDMA is strongly correlated. This is the case also in urban radio environments and despite of large duplex separation of W-CDMA.

Therefore, the utilization of spatial information derived during uplink reception for downlink beamforming purpose makes sense. As a consequence, adaptive antenna downlink beamforming without terminal feedback is possible also in urban radio environments.

## REFERENCES


[1] A. J. Paulraj, C. B. Papadias, "*Space-Time Processing for Wireless Communications*", IEEE Signal Processing Magazine, No. 6, Vol. 14, pp. 49-83, November 1997.

[2] A. Kuchar, M. Tangemann, E. Bonek, "*A Real-Time DOA-Based Smart Antenna Processor*", IEEE Transactions on Vehicular Technology, to be published.

[3] L. Bigler, H. P. Lin, S. S. Jeng and G. Xu, "*Experimental Direction of Arrival and Spatial Signature Measurements at 900 MHz for Smart Antenna Systems*", Proc. IEEE VTC'95, Vol. 1, pp. 55-58, Chicago, USA (1995).

[4] K. I. Pedersen, P. E. Mogensen, F. Fredriksen, "*Joint-Directional Properties of Uplink and Downlink Channel in Mobile Communications*", Electronic Letters, Vol. 35, No. 16, pp. 1311-1312, 5. August 1999.

[5] B. H. Allen, "*Smart Antennas for High Data Rate FDD Wireless Links*", Dissertation, University of Bristol, Bristol, UK, April 2001.

[6] S. E. Foo, et. al., "*Frequency Dependency of Spatial-Temporal Characteristics of UMTS FDD links*", COST 273 TD(02)027, Guildford, UK, January 2002.

[7] B. Fleury, D. Dahlhaus, R. Heddergott, M. Tschudin, "*Wideband Angle of Arrival Estimation Using the SAGE Algorithm*", Proc. IEEE ISSSTA'96, pp. 79-85, Mainz, Germany (1996).

[8] M. Haardt, J. A. Nossek, "*Unitary ESPRIT: How to Obtain Increased Estimation Accuracy with a Reduced Computational Burden*", IEEE Transactions on Signal Processing, Vol. 43, No. 5, pp. 1232-1242, May 1995.

[9] M. Bartlett, "*Smoothing Peridiograms from Time Series with Continuous Spectra*", Nature, No. 161, 1948.

[10] Personal communication between Klaus Hugl and Sze Ern Foo, January 2002.

[11] PROPSound Radio channel sounder home page of Elektrobit AG. Available at http://www.elektrobit.ch/propsound/.

[12] K. Kalliola, P. Vainikainen, "*Characterization System for Radio Channel of Adaptive Array Antennas*", Proc. IEEE PIMRC'97, pp. 95-99, Helsinki, Finland (1997).

[13] K. Hugl, "*Spatial Channel Characteristics for Adaptive Antenna Downlink Transmission*", Dissertation, 192p., Institut für Nachrichtentechnik und Hochfrequenz-technik, Technische Universität Wien, January 2002. available at: www.nt.tuwien.ac.at/mobile/theses_finished

[14] J. Bach Andersen, K.I. Pedersen, "*Angle-of-arrival statistics for low angular resolution*", Proc. EPMCC'2001, Vienna, Austria (2001).

[15] K. Hugl, K. Kalliola, J. Laurila, "*Spatial Channel Characteristics for Macro- and Microcellular BS Installations*", Proc. COST 273 Workshop on "Opportunities of the Multidimensional Propagation Channel", Espoo, Finland (May 29-30, 2002).

[16] J. Capon, R. J. Greenfield, R. J. Kolker, "*Multidimensional Maximum-Likelihood Processing of a Large Aperture Seismic Array*", Proceedings of IEEE, Vol. 55, pp. 192-211, February 1967.